DESIGN AND MODELLING OF A METASURFACE FOR LOW-FREQUENCY ROOM MODE ABSORPTION

Juan L. de la Torre[1], Eduardo Latorre Iglesias[1], Yingyao Xiong[1], Aurora Melis[1], M. López Ibáñez[1], Francisco Aznar Ballesta[2], Marta Gil Barba[2]

[1] *Grupo de Investigación en Acústica Arquitectónica, Universidad Politécnica de Madrid, Madrid, Spain*
[2] *Desarrollo e Investigación Electromagnética, Universidad Politécnica de Madrid, Madrid, Spain*

Abstract

Low-frequency room modes remain a major challenge in architectural acoustics, as they cannot be effectively mitigated using conventional absorbers or resonators without a significant thickness. As an alternative, acoustic metamaterials offer the possibility of achieving efficient low-frequency absorption with limited thickness. A numerical methodology for the design and optimisation of a spiral metasurface aimed at room mode control is presented. A finite element model of a rectangular enclosure is implemented in COMSOL Multiphysics and adjusted using measurements. Based on the modal characteristics of the room, a spiral labyrinth structure is designed and tuned to target a specific low-frequency mode. Analytical and numerical simulations are conducted to evaluate the absorption performance of the spiral metasurface and to optimise both its internal geometry and its spatial distribution within the enclosure. The selected geometries are then 3D printed and their performance is assessed experimentally using an impedance tube. The good agreement between numerical simulations and measurements exhibits the potential of this approach as a tool for acoustic metamaterial design for room-mode control. The observed amplitude reduction of the selected room mode shows that metasurfaces based on labyrinth structures are an effective and scalable solution for low-frequency modal control in enclosures, overcoming the limitations of traditional absorptive materials.

Keywords: metasurface, room modelling, low-frequency absorption, room modes

Corresponding author: *juanluisdela.torre.moral@upm.es.*

1. Introduction

Low-frequency room modes produce uneven sound pressure distributions and degrade room acoustic quality. Conventional treatments, including porous absorbers, Helmholtz resonators and panel absorbers, require large volumes to achieve effective low-frequency absorption, limiting their practical application. Acoustic metasurfaces provide subwavelength control of sound through resonant structures whose response is determined by their geometry [1], [2], [3]. Unlike conventional absorbers, they can achieve efficient low-frequency absorption with substantially reduced thickness, making them attractive where installation space is limited [4], [5]. The metasurfaces developed in this work employ an embedded channel whose length and cross-sectional area are selected to achieve narrow-band absorption through quarter-wavelength resonances. A design methodology combining analytical modelling, finite-element simulations and experimental validation is proposed for low-frequency room mode control. The analytical model describes acoustic propagation in narrow channels [6], incorporating thermoviscous losses using canonical formulations for circular [7] and rectangular ducts [8]. The metasurface was designed to target the first tangential mode of a small enclosure ($1.44 \times 0.91 \times 1.64$ m). The enclosure response was first measured at four corner positions to identify its low-frequency resonances. The analytical and numerical models were validated through impedance tube measurements of the absorption coefficient of 3D-printed samples. Finally, 48 metasurface units were installed in the enclosure to evaluate their effectiveness for room mode attenuation and to validate the numerical enclosure model.

2. Models to predict the absorption coefficient of the metasurface

To predict the absorption coefficient of the designed metasurface both analytical and numerical models are used. The first allows quick calculations to adjust the metasurface channel length and cross-sectional area to fit the frequency of maximum absorption to the desired value. The second allows more detailed geometries and greater geometric complexity to be considered in the calculations, while also ensuring that the analytical model fully accounts for the underlying physics of the problem.

2.1. Analytical model

The acoustic channel of the metasurface was analytically modelled as a narrow rectangular duct with a rigid end and of length L, width a_x, height b_y and cross-sectional area $S_r = a_x b_y$. Viscous and thermal boundary-layer effects are included using the formulation derived by Stinson for thermo-viscous propagation in ducts of arbitrary cross-section [8].

The ambient fluid properties used in the model are the static pressure P_0, the temperature T, the ratio of specific heats γ, the gas constant R_{gas}, the dynamic viscosity μ, the Prandtl number Pr, and the specific heat at constant pressure c_p. From these quantities, the air density and the sound speed are obtained as $\rho_0 = P_0/(R_{\text{gas}}T)$ and $c_0 = \sqrt{\gamma P_0/\rho_0}$. The kinematic viscosity is defined as $\nu = \mu/\rho_0$, and the thermal diffusivity is $\nu_p = \kappa/(\rho_0 c_p)$, where $\kappa = (\mu c_p)/Pr$ represents the thermal conductivity.

Following the Stinson formulation [8], the viscous and thermal correction functions are obtained from a modal summation over the transverse modes of the rectangular duct, where $\omega = 2\pi f$ is the angular frequency. In this implementation, half-width and half-height are defined as $a = a_x/2$ and $b = b_y/2$. Defining $\alpha_k = ((k + 1/2)\pi)/a$ and $\beta_n = ((n + 1/2)\pi)/b$, the generic correction function is:

$$F(\omega, \eta) = \frac{4i}{\eta a^2 b^2} \sum_{k=0}^{\infty} \sum_{n=0}^{\infty} \frac{1}{\alpha_k^2 \beta_n^2} \frac{1}{\alpha_k^2 + \beta_n^2 + i\omega/\eta}. \quad (1)$$

where η is a diffusivity parameter. For the viscous correction function, $\eta = \nu$, whereas for the thermal correction function, $\eta = \nu_p/\gamma$.

The viscous and thermal functions are $F_v = F(\omega, \nu)$ and $F_t = F(\omega, \nu_p/\gamma)$. In the numerical implementation, both summations were truncated to $K_{\max} = 60$ and $N_{\max} = 60$, which ensured convergence over the analysed frequency range. The effective density is $\rho_{\text{eff}} = \rho_0/F_v$, and the compressibility by

$$C_{\text{eff}} = \frac{1}{\gamma P_0} \left[\gamma - (\gamma - 1)F_t\right]. \quad (2)$$

From these effective properties, the complex wavenumber and characteristic impedance are $k_c = \omega\sqrt{\rho_{\text{eff}} C_{\text{eff}}}$ and $Z_c = (1/S_r)\sqrt{\rho_{\text{eff}}/C_{\text{eff}}}$. Assuming rigid termination, the surface acoustic impedance of the rectangular channel is

$$Z_s = -iZ_c \cot(k_c L). \quad (3)$$

To evaluate its response under normal incidence, the device is coupled to an impedance tube of diameter D_0, with cross-sectional area $S_0 = \pi(D_0/2)^2$. The characteristic impedance of the impedance tube is $Z_0 = (\rho_0 c_0)/S_0$, and the reflection coefficient is $R = (Z_s - Z_0)/(Z_s + Z_0)$. The normal-incidence absorption coefficient can be obtained as

$$\alpha = 1 - |R|^2. \quad (4)$$

2.2. Numerical model

Numerical simulations based on FEM are performed alongside the analytical model. These simulations provide a more detailed analysis of the acoustic behaviour inside the metasurface under different environments or conditions. The software used for this purpose is COMSOL Multiphysics. The metasurface Computer-Aided Design (CAD) geometry is imported into COMSOL Multiphysics and coupled to a cylindrical domain that represents the assembly between an impedance tube and the metasurface. The Pressure Acoustics module is used for the full acoustic domain, where the Narrow Region Acoustics option is used to specify thermo-viscous losses in the metasurface channel.

The finite element mesh is generated using a maximum element size of $\lambda/6$ for the highest frequency of interest, which in this case is 200 Hz. Due to the complexity of the channel geometry, the mesh is manually adjusted to avoid meshing conflicts in areas of the model with small details. A finer mesh is required in the channels to reproduce their geometry with sufficient precision, whereas a coarser mesh can be used in the air domain inside the impedance tube.

The frequency range of study is defined in the Pressure Acoustics module by specifying a starting frequency of 100 Hz, an ending frequency of 200 Hz, and a frequency step of 0.5 Hz. The acoustic channel cross-section and dimensions are defined in the Narrow Acoustic module. An excitation port, using a pressure amplitude of 1 Pa, is defined at the entrance of the impedance tube, on the opposite side of the position of the sample.

Similarly to Equation 4, the absorption coefficient is calculated using the power balance at the excitation port:

$$\alpha = \frac{W_{\text{i}} - W_{\text{r}}}{W_{\text{i}}} = 1 - \frac{W_{\text{r}}}{W_{\text{i}}}, \quad (5)$$

where W_{i} and W_{r} are the incident and reflected sound power at the input port of the impedance tube.

3. Experimental characterization of the enclosure

The rectangular enclosure shown in Figure 2 (left) with dimensions $L_x = 1.44\,\text{m}$, $L_y = 0.91\,\text{m}$, and $L_z = 1.64\,\text{m}$ was chosen for this study. The enclosure was constructed using rigid wood panels for walls, floor and ceiling. To obtain frequency responses inside the enclosure, a speaker was placed on the floor close to one of the corners, and four microphones were placed in the positions defined in Table 1, with the bottom left corner as origin of coordinates, as shown in Figure 2. The experimental setup consisted of two

Brüel & Kjær 4189 microphones, a Yamaha MSP5 loudspeaker and a MOTU UltraLite-mk3 audio interface, with signal generation and acquisition performed using SpectraPLUS. The excitation process was carried out using a logarithmic frequency sweep from 50 to 400 Hz with a duration of 20 seconds. The measured frequency responses at the measurement points, used to identify the first resonance frequencies of the enclosure, are shown in Figure 1. The response is shown in decibels, but normalised to the maximum value obtained over the entire frequency range for all measurements. The third mode at 167 Hz is dominant and is easily identifiable for all microphone positions, so it is chosen as the target mode to be attenuated. This mode is identified as the first tangential mode $(1, 0, 1)$, and its corresponding mode shape is presented in Figure 2, where the maximum sound pressure is identified close to the short edges of the enclosure, and the minimum sound pressure is found in the centre of the enclosure surfaces.

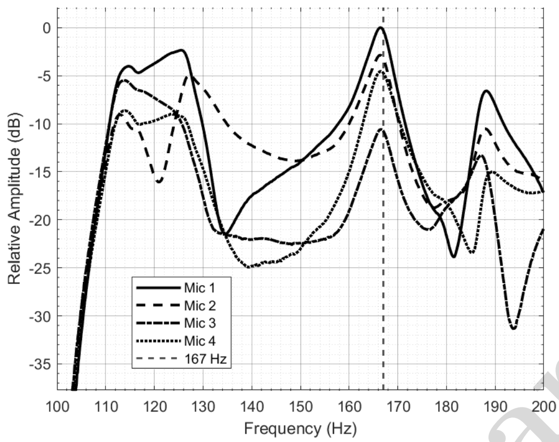

Figure 1: Frequency response of the empty enclosure measured in four microphone positions.

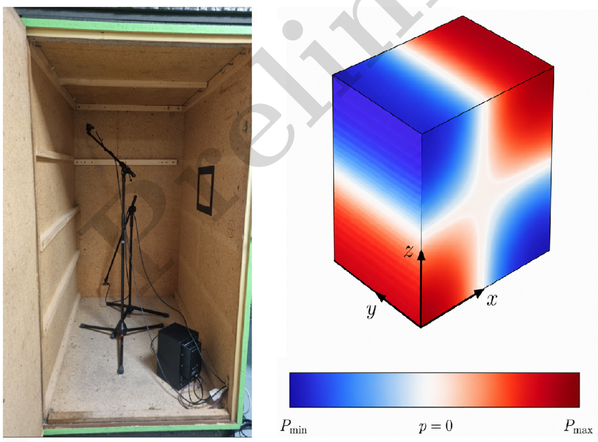

Figure 2: Enclosure used in this study (left) and mode shape of the targeted tangential mode $(1, 0, 1)$ at 167 Hz (right).

Table 1: Coordinates inside the enclosure of the microphone and speaker positions used during frequency response measurements. Origin of coordinates defined in the bottom left corner of the enclosure, as shown in Figure 2.

Position	X (m)	Y (m)	Z (m)
Mic 1	1.35	0.70	0.15
Mic 2	1.29	0.81	1.52
Mic 3	0.85	0.37	0.21
Mic 4	0.31	0.53	1.42
Speaker	0.35	0.15	0.08

4. Metasurface design, fabrication and characterization

4.1. Design and fabrication

A metasurface was designed using the analytical model described in section 2.1, aiming at a maximum absorption frequency of 167 Hz. The required channel length is 504 mm. To accommodate this length within a compact volume, the channel was embedded within a solid structure following an Archimedean spiral layout. The analytical model predicts that the maximum absorption coefficient is achieved for a square channel cross-section with a side length of 13.3 mm. The thickness of the metasurface is 16 mm. Square and rectangular channel cross-sections allow for more efficient use of the metasurface volume than circular cross-sections, so a rectangular cross-section is chosen. A CAD model of the resultant device following these design constraints is shown in Figure 3, along with an extension for the unit entrance, whose purpose is explained in section 4.2.

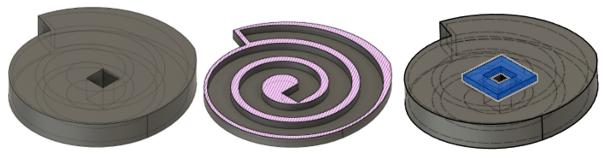

Figure 3: Spiral metasurface CAD design: general view (left), cross-section view (middle), extension (right).

Metasurface samples were fabricated by fused deposition modelling (FDM) using a Bambu Lab X1 Carbon 3D printer and polylactic acid (PLA) filament. A nozzle diameter of 0.4 mm and a layer height of 0.2 mm were used. The fabrication time was approximately 90 min per unit.

4.2. Experimental characterization and adjustment

To validate the results obtained from the analytical model, the sound absorption coefficient of a metasurface sample was experimentally characterised using an impedance tube following the two-microphone transfer-function method according to ISO 10534-2 [9]. The impedance tube employed has a circular section of 100 mm diameter and 1 m of length. The results, shown in Figure 4, reveal a discrepancy between the analytical predictions and the measurements. A difference of approximately 2 Hz was observed in the maximum absorption frequency between the measured sample and the analytical prediction. This mismatch may be caused by the right-angle bend at the channel entrance or surface roughness, whose associated losses are not accounted for in the analytical model. Furthermore, the measured absorption coefficient was approximately 0.08 lower than that predicted by the analytical model. A better agreement with the measurements was obtained in the FEM model.

To correct this frequency mismatch, an extension piece was manufactured and attached to the channel entrance, increasing the channel length from 504 mm to 508 mm, adjusting the measured maximum absorption frequency from 169 Hz to the target frequency of 167 Hz. This modification is shown in Figure 3 (right).

The measurements and numerical simulations of the modified device demonstrate the effectiveness of this adjustment. The maximum absorption frequency was successfully reduced by approximately 2 Hz through the increase in the acoustic path length provided by the extension piece. However, the measured absorption coefficient was slightly lower than that obtained for the original configuration. In contrast, the FEM predicted a slight increase in absorption while reproducing the desired frequency shift.

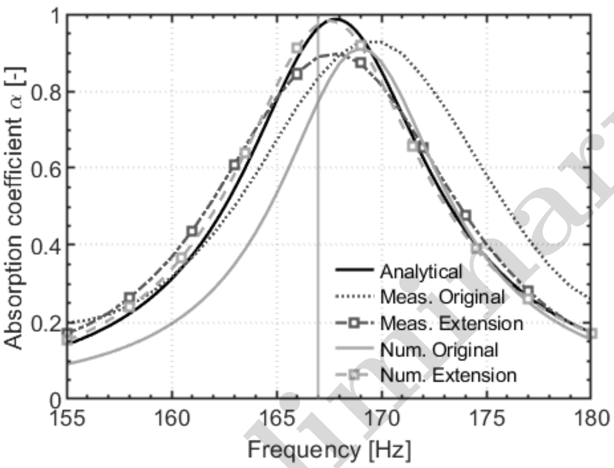

Figure 4: Absorption coefficient obtained with the original metasurface design and modified with an extension piece attached to the channel entrance. Results show analytical and numerical predictions and measurements.

5. Evaluation of the metasurface inside the enclosure

To assess the effect of the metasurface designed following the steps given in Section 4 on the sound field inside the enclosure, a numerical model in COMSOL Multiphysics is developed. The designed metasurface is imported into the model and the frequency response is predicted for the empty enclosure and for several configurations with metasurface units installed. An experimental study is also performed after 3D printing 48 units of the designed metasurface.

5.1. Numerical simulations

To assess the feasibility of the metasurface to reduce the amplitude of the modal response of the enclosure, numerical simulations were carried out. A model of the enclosure was developed in COMSOL Multiphysics and 48 units of the designed metasurface were included, with two rows of 6 units placed along the four short edges of the enclosure. The modelled enclosure is the same as in section 3, with receivers placed at the same positions as those listed in Table 1, and the excitation generated by a monopole source located at the speaker coordinates. Although the impedance of the enclosure surfaces is not adjusted to match the impedance of the wood panels (rigid boundaries were chosen instead), the results can provide insights into the acoustic behaviour of the metasurface placed inside the enclosure. A more refined mesh is required to accurately reproduce the metasurface geometry, compared to the coarser mesh used for the enclosure.

Figure 5 shows that, for a sinusoidal excitation of 167 Hz, the sound pressure level in the channels of the metasurfaces is maximum, showing their resonant behaviour. In addition, the minimum sound pressure areas are located in the centre of the enclosure surfaces.

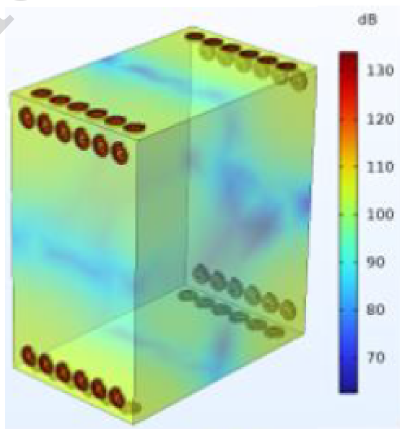

Figure 5: Numerical model in COMSOL Multiphysics of 48 units of metasurfaces placed along the short edges of the enclosure. The colour map shows sound pressure levels.

Looking at the frequency responses calculated in Microphone 1 shown in Figure 6, the simulations predict a reduction of up to 19 dB in the peak related to the chosen tangential mode, as well as a slight shift (2 Hz) to higher frequencies of the modal peak when the metasurfaces are included. In addition, it can be seen that the peak frequency with the empty room is 160 Hz, which is 7 Hz lower than the frequency obtained in the measurements. This difference is probably due to the use of a totally rigid boundary condition in the enclosure surface, which shows the need to adjust the surface impedance to obtain more accurate results.

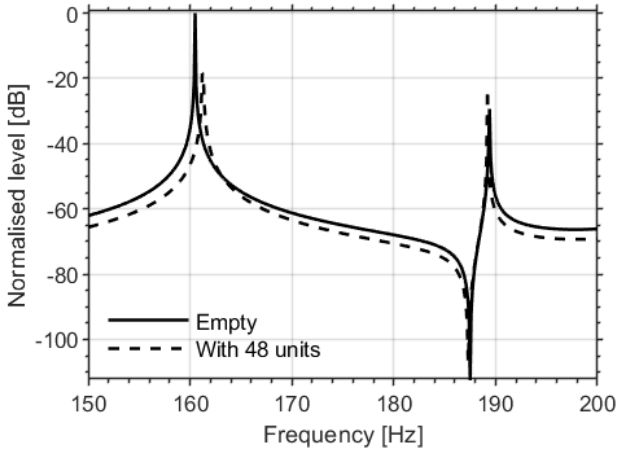

Figure 6: Numerical simulation of the room frequency response in Microphone 1. Continuous line: Empty enclosure. Dashed line: Enclosure with 48 units distributed among the enclosure short edges. 12 units were placed along each edge, with two rows of 6 units on each side.

5.2. Experimental characterization

Next, an evaluation of the performance of the designed metasurface is performed experimentally for different configurations inside the enclosure. The frequency response was measured following the same procedure described in section 3. The results are normalized using the maximum value in the entire frequency range as a reference.

Two sets of measurements were performed. In the first, the original metasurface design (without the frequency tuning extension) was evaluated by progressively increasing the number of units installed along one of the short edges of the enclosure. Four configurations were tested, comprising 12, 24, 36 and 48 units, as shown in Figure 7 (left).

In the second set of measurements, the frequency tuning extension was attached to all 48 metasurface units. An example of a unit with the extension piece is shown in Figure 3. The 48 adjusted units were then distributed around the enclosure, with two rows of six units installed on each of the four edges, as shown in Figure 7 (right).

5.3. Results

The results for the first set of measurements are shown in Figure 8 for Microphone 1. Two rows of six units are first placed on both sides of a short edge of the enclosure, as shown in Figure 7 (left), for a total of 12 units. Additional rows of six units are added for a total of 24, 36 and 48 units so that each added row is positioned farther from the edge than the previous one. Increasing the number of units leads to higher attenuation. However, the improvement becomes significantly less pronounced when subsequent rows of units are added than when the first two rows were included. At 167 Hz, an attenuation of 6 dB is obtained when 12 units are added. When more rows are added to have 24, 36 and 48 units, the relative attenuation

Figure 7: Distribution of the metasurface units inside the enclosure for evaluation of sound reduction. Left: 48 units placed on both sides of one short edge of the enclosure. Right: Two rows of 6 units are placed on both sides of each enclosure short edge.

obtained is 3 dB, 1 dB and 1.5 dB, respectively, for a total attenuation of 11.5 dB with 48 units compared to the empty enclosure. It can also be observed that a maximum attenuation of 14 dB is obtained at 169 Hz, which is the maximum absorption frequency of the 3D printed metasurface based on the original design. Although the absorptive effect is maintained, the maximum attenuation does not occur exactly at the modal frequency.

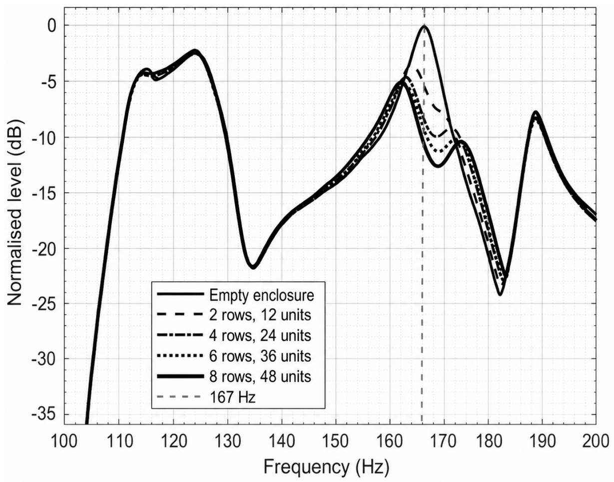

Figure 8: Measured frequency responses for increasing number of rows of 6 metasurfaces in one enclosure short edge.

For the metasurfaces with the extension piece added at the channel entrance, the achieved attenuation, expressed as the difference between the measured frequency response for the empty enclosure and with 48 metasurfaces, is presented in Figure 9, for four microphone positions. Its average is also included. The attenuation at 167 Hz varies from 13 to 15 dB between microphone positions. The maximum reduction occurs at the frequency of the chosen tangential mode.

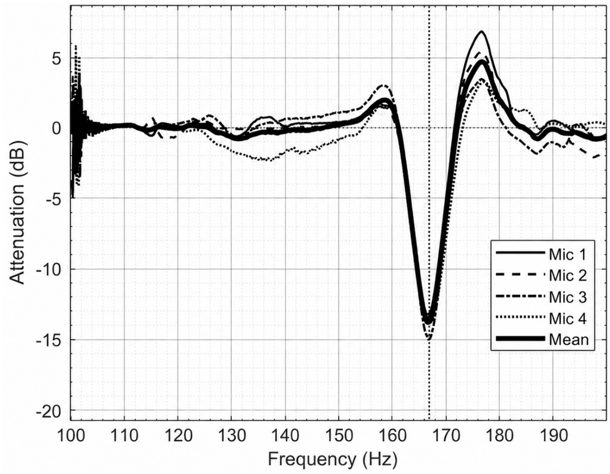

Figure 9: Attenuation with 48 metasurface units (Tuned with the extension piece), placed on every enclosure short edge, measured in four microphone positions.

6. Conclusions and further work

This work investigates the application of acoustic metasurfaces to attenuate low-frequency room modes. A methodology for their design is proposed, which combines analytical and numerical predictions and measurements in an impedance tube. The metasurface geometry was adjusted to attenuate the response of the first tangential mode of a small enclosure. A finite element model of the enclosure is used to assess the effect of the designed metasurface on reducing the mode response. 48 units of the metasurface were 3D printed and installed inside the enclosure in different configurations to evaluate their effect on the sound field.

Using 48 metasurfaces, reductions of approximately 14 dB were achieved at the targeted modal frequency (167 Hz). Their spatial distribution is relevant to their performance. Placing the units in regions of high sound pressure close to the short edges of the enclosure is important to maximise absorptive effects. An accurate adjustment of the maximum absorption frequency to the modal frequency was also important, although small frequency deviations still provided substantial attenuation.

Future work will focus on optimising the spatial distribution of the metasurface units inside the enclosure according to the mode shape of the targeted mode, for axial, tangential, and oblique modes. In addition, corrections to the analytical model should be introduced to account for the effect of corners or bends on the effective length of the channel. For the numerical model of the enclosure, adjustment of the surface impedance and a more accurate sound source modelling will also be pursued. Further parametrisation and optimisation of the metasurfaces will be investigated to enhance both the absorption frequency bandwidth and the overall efficiency.

7. Acknowledgments

This work has been supported by the Madrid Government (Comunidad de Madrid-Spain) under the Multiannual Agreement 2023-2026 with Universidad Politécnica de Madrid in the Line A, Emerging PhD researchers.

References

[1] Z. Liu et al., "Locally resonant sonic materials," *Science*, vol. 289, no. 5485, pp. 1734–1736, 2000. DOI: 10.1126/science.289.5485.1734.

[2] J. Mei, G. Ma, M. Yang, Z. Yang, W. Wen, and P. Sheng, "Dark acoustic metamaterials as super absorbers for low-frequency sound," *Nat. Commun.*, vol. 3, p. 756, 2012. DOI: 10.1038/ncomms1758.

[3] K. Donda, Y. Zhu, S. Fan, L. Cao, Y. Li, and B. Assouar, "Extreme low-frequency ultrathin acoustic absorbing metasurface," *Appl. Phys. Lett.*, vol. 115, no. 17, p. 173 506, 2019. DOI: 10.1063/1.5126024.

[4] C. Zhang and X. Hu, "Three-dimensional single-port labyrinthine acoustic metamaterial: Perfect absorption with large bandwidth and tunability," *Phys. Rev. Appl.*, vol. 6, no. 6, p. 064 025, 2016. DOI: 10.1103/PhysRevApplied.6.064025.

[5] A. Dalvand, R. Hedayati, S. Azadi, and A. Jafari, "Thin labyrinthine acoustic metamaterials for firewall to attenuate interior noise in automobile," *Results Eng.*, vol. 32, p. 111 594, Jun. 2026. DOI: 10.1016/j.rineng.2026.111594.

[6] N. Jimenez, O. Umnova, and J.-P. Groby, *Acoustic Waves in Periodic Structures, Metamaterials and Porous Media: From Fundamentals to Industrial Applications.* Springer, 2021. DOI: 10.1007/978-3-030-75868-3.

[7] C. Zwikker and C. W. Kosten, *Sound Absorbing Materials.* New York: Elsevier, 1949.

[8] M. R. Stinson, "The propagation of plane sound waves in narrow and wide circular tubes and generalization to uniform tubes of arbitrary cross-sectional shape," *J. Acoust. Soc. Am.*, vol. 89, no. 2, pp. 550–558, 1991. DOI: 10.1121/1.400379.

[9] *Iso 10534-2:2023 acoustics—determination of acoustic properties in impedance tubes—part 2: Two-microphone technique for normal sound absorption coefficient and normal surface impedance*, Geneva, Switzerland: International Organization for Standardization, 2023.